Disruption of the eIF2α-P stress response rheostat evokes dystonia-like movements

Sara A. Lewis[1,2], Jacob Forstrom[1,2], Jennifer Tavani[1,2], Sergio R. Padilla-Lopez[1,2], Michael C. Kruer[1,2,3]

For submission to Neuron

Affiliations:

1 Barrow Neurological Institute, Phoenix Children's Hospital, Phoenix, AZ, USA

2 Departments of Child Health, Cellular & Molecular Medicine, Genetics, and Neurology, University of Arizona College of Medicine - Phoenix, Phoenix, AZ, USA

3 Programs in Neuroscience, Molecular & Cellular Biology, and Biomedical Informatics, Arizona State University, Tempe, AZ USA

Sara A Lewis	gaugers@arizona.edu
Jacob Forstrom	jacobforstrom@arizona.edu
Jennifer Tavani	jrtavani@arizona.edu
Sergio R. Padilla-Lopez	spadillalopez@arizona.edu
Michael C. Kruer	kruerm@arizona.edu

Summary

Dystonia is the 3rd most common movement disorder, typified by twisting and/or posturing movements. The molecular and cellular mechanisms connecting genetic and environmental insults to altered brain circuit connectivity and dystonia are not known. In dystonia models and in response to stress, eIF2α is phosphorylated (eIF2α-P) to decrease global protein translation and upregulate plasticity and stress-response genes, but whether eIF2α-P can directly alter motor circuit properties is unknown. Here, we test whether increases/decreases of eIF2α-P can affect motor function and connectivity in a Drosophila model. We find altering eIF2α-P in either direction produces abnormal posturing and disordered movements in flies, recapitulating the dystonia-like dyskinetic movements previously observed in the DYT1 fly model. We identify cell type specificity of dystonia-like movements in response to heat and mechanosensory stimulation. Finally, we observe increased synaptic connectivity with increased eIF2α-P, linking molecular alterations to changes in circuit connectivity driving unwanted muscle activation and dystonia.

Keywords (10)

dystonia, ISR, eIF2alpha, Drosophila, acetylcholine, D2 receptor, ISRIB, DYT1, PEK, PPP, synaptic plasticity

Introduction

Eukaryotic initiation factor (eIF2) is the protein translation complex that brings initiator tRNA, mRNA, and the ribosome together for protein translation under basal conditions (Sonenberg and Hinnebusch, 2009). Phosphorylation of the eIF2 alpha subunit (eIF2α-P) regulates protein translation as part of the integrated stress response (ISR) (Pakos-Zebrucka et al., 2016). eIF2a can be phosphorylated by kinases regulated by diverse cytotoxic stressors, including the kinase GCN2 (which senses essential amino acid deprivation) (Kilberg et al., 2009), PKR (which is activated by virus-associated dsRNA) (García et al., 2007), HRI (a heme-regulated inhibitor activated by oxidative stress, cytoplasmic protein aggregates, and nitric oxide signaling) (Girardin et al., 2021), and PEK (which senses ER stress from unfolded protein accumulation) (Ron and Walter, 2007). In response to cellular signals, eIF2α phosphorylation selectively regulates mRNA translation. Most human transcripts contain an upstream open reading frame out of frame with the canonical coding sequence (Calvo et al., 2009). Although most uORFs serve to inhibit sequence affinity for the ribosome when eIF2α is phosphorylated (Young and Wek, 2016) resulting in a global decrease in protein synthesis, a distinct class of uORFs are preferentially upregulated by eIF2α-P. eIF2α-P increases expression of the transcription factor ATF4 which regulates expression of the apoptosis factor CHOP, the protein chaperone BiP, autophagy components, (Neill and Masson, 2023). ATF4 is also a known inhibitor of CREB-mediated neuronal plasticity (Smith et al., 2020), with additional roles in regulating receptor trafficking (Corona et al., 2018), postsynaptic maturation (Liu et al., 2014), and other long term depression (LTD) or long term potentiation (LTP) factors as part of neuronal plasticity (Chesnokova et al., 2017). High levels of ATF4 initiates negative feedback to reset the pathway by increasing expression of the growth arrest and DNA damage-inducible protein (GADD34/PPP1R15). The regulatory subunit 15A of this phosphatase removes the phosphate group from eIF2α (Malzer et al., 2013).

eIF2α-P serves as a biological rheostat by dynamically regulating protein translation based upon cellular supply and demand. This phosphorylation is intricately controlled, with dysregulation in either direction disrupting cellular function. Sustained phosphorylation of eIF2α can result in significant downregulation of the rate of protein synthesis (Clemens, 2005) and more severe ATF4-mediated responses including apoptosis (Neill and Masson, 2023). In contrast, abnormally decreased phosphorylation can fail to activate responses to stress and can worsen function after traumatic brain injuries (Valenzuela et al., 2016 ; Wang et al., 2019).

There is also mounting evidence that eIF2α-P translational regulation is an important regulator of synaptic plasticity in the absence of stress, and dysregulated eIF2α-P could be a feature of numerous neurological conditions (Chesnokova *et al.*, 2017)

Dystonia is a disabling neurological disorder and is the third most common movement disorder behind Parkinson Disease and essential tremor. Dystonia is a form of dyskinesia, or abnormal, involuntary movements, that is exemplified by twisting and/or posturing movements. Dystonia can be focal or generalized and can be relatively constant (e.g. tonic) or intermittent (e.g. phasic, task specific) (Balint et al., 2018). Dystonia may respond to medications, injection therapies (botulinum toxins or phenol), or deep brain stimulation but it is often painful for affected individuals and refractory to medical treatment. No new dystonia treatments have been developed for decades, and although advances have been made in our understanding of dystonia at the genetic and circuit levels, progress in the field has been hampered by our limited knowledge of the molecular and cellular substrate of dystonia that connects genetic and circuit observations.

Dysfunction of ISR and eIF2α-P has been increasingly linked to multiple dystonia etiologies. Mutations in the eIF2α-P kinases PKR*/EIF2KA2* (Kuipers et al., 2021; Mao et al., 2020) HRI/*EIF2KA1* (Mao *et al.*, 2020) and upstream activating kinase *PRKRA/DYT16,* (Zech et al., 2014) represent monogenic causes of dystonia. Abnormalities of the eIF2α-P axis have also been observed in models of genetic dystonia, albeit indirectly in some cases. Increasing eIF2α-P improved localization phenotypes in *DYT1* patient cells and defective LTD in *DYT1* mice (Rittiner et al., 2016). Although ATF4 expression was poorly upregulated in response to stress in *DYT1* patient cells compared to controls, (Rittiner *et al.*, 2016), ISR components were upregulated at baseline in a *DYT1* rat model (Beauvais et al., 2016). Increased expression of ISR components, including ATF4, was also observed in a *DYT6* rat model (Zakirova et al., 2018). Finally, blocking physiologic eIF2α-P activation during the initial response to hypoxia-ischemic and traumatic brain injuries (each of which can induce dystonia) exacerbates injury and lead to worse outcomes in mouse models (Valenzuela *et al.*, 2016 ; Wang *et al.*, 2019). However, unchecked chronic eIF2α-P activation may also be detrimental. Inhibition of chronic eIF2α-P pathway activation after the initial response can improve TBI model outcomes (Chou et al., 2017).

Whether changes in eIF2α-P drive the development of dystonia, play a compensatory role, or represent a nonspecific downstream finding is unknown. In our recent studies of the fly ortholog of the dystonia-associated gene *AGAP1*, we found that basally elevated eIF2α-P in mutants was associated with an inability to further increase phosphorylation when confronted

with unfolded protein or starvation stressors (Lewis et al., 2023). This suggests that genetic predispositions to dystonia can elevate baseline ISR responses as a compensatory response, disrupting normal physiology and limiting cells' ability to respond to a second hit, leaving them more susceptible to subsequent injury.

Currently, it is not known how changes in neuron or circuit properties arise in dystonia, leading to altered connectivity between sensory-motor cortex, thalamus, cerebellum, and basal ganglia (Niethammer et al., 2011 ; Vo et al., 2015). Possible candidates include altered synaptic connectivity, neuronal hyperexcitability, or changes in synaptic strength. Synaptic connectivity changes have been observed as increased medium spiny neuron dendrite arbor size in a *DYT1* knock-in mouse model (Song et al., 2013). Alterations in neuron excitability have been observed, with decreased firing of striatal neurons of the indirect pathway in a paroxysmal dyskinesia (PNKD) mouse model during dyskinesia bouts (Nelson et al., 2022). Increased synaptic plasticity via excessive LTP and impaired LTD have been observed in several dystonia models (Maltese et al., 2018 ; Zakirova *et al.*, 2018). However, these observations have been made in different models and different contexts, and not directly connected in a linear fashion.

Striatal cholinergic neurons and neurons expressing D2 receptors in the indirect motor pathway have both been implicated in the cellular origin of dystonia, although the exact neurobiology of dystonia is unknown. Anticholinergic medications can treat dyskinetic symptoms and dopamine antagonists can both treat dyskinesias/dystonia and induce dyskinetic movements with long-term use (Calabresi and Standaert, 2019; Thenganatt and Jankovic, 2014). Striatal cholinergic neurons are both increased in size (Song *et al.*, 2013) and more excitable (Eskow Jaunarajs et al., 2015) in rodent models of *DYT1* dystonia. Acetylcholine is known to increase the release of dopamine in the striatum (Zhou et al., 2001). There is reduced D2 receptor binding in various forms of isolated idiopathic dystonias detected by PET radioimaging (Karimi and Perlmutter, 2015). Together, this suggests a model where acetylcholine positively regulates dopamine levels, inhibiting D2-receptor expressing neurons, and thereby preventing unwanted movements.

Animal models of dystonia have been developed in mice, rats, and flies. We utilized Drosophila as a genetically tractable model given that prior work has established that transgenic *DYT1* flies exhibit dystonia-like dyskinetic movements (Koh et al., 2004). We systematically tested whether altering eIF2α phosphorylation can disrupt normal neuromotor function and which cell types are sensitive to eIF2α-P alterations. We establish both increases and decreases in eIF2α phosphorylation as a model for dystonia in flies which recapitulates core

features of the disorder. We also identify eIF2α-P changes as a potential driver of dystonia with a potential role for decreasing neurotransmission and increasing synaptic connectivity.

Results

Genetic modification of eIF2α phosphorylation impairs locomotion

We utilized a Drosophila fly model to first examine the role of eIF2α-P in locomotion. We started with whole animal partial loss-of-function alleles of a major eIF2α kinase (PEK; to increase) and phosphatase (PPP1R15A; to decrease) eIF2α-P (**Fig.1 A**). We confirmed altered eIF2α-P with these genetic manipulations to PPP (**Table 1**) and PEK (**Table 2**) via western blotting (**Supplemental Figure 1**). We identified a decrease in distance traveled in a climbing assay in homozygotes with both PPP (**Fig. 1B**) and PEK loss of function alleles (**Fig. 1C**). We confirmed that these phenotypes originate from neurons by using the ELAV pan-neuronal Gal4 driver for cell-type specific overexpression of both eIF2α-P kinase and phosphatase. We found that overexpression of either PPP1R15 (PPP) or kinase (PEK) decreased distance traveled (**Fig. 1D-E**). This demonstrates that increased or decreased eIF2α-P levels alone are sufficient to cause locomotor impairments. This is consistent with the model that eIF2α maintains an ideal range of phosphorylation. We reproduced impairments in the locomotor assay with overexpression of the downstream target of eIF2α-P, ATF4 (**Fig. 1F**), suggesting that this phenotype may be attributable to expression of stress response or LTP/LTD genes.

Locomotor impairments resulting from decreased eIF2α-P can be induced in either neurons or glia, with cell-type dependent effects

We utilized Gal4 lines with different cell-type, neurotransmitter, and regional specificity to map the origin of the movement phenotype. Based on findings that the pan-neuronal driver ELAV impaired locomotion when PPP is overexpressed (**Fig. 2A**), we first confirmed this in a second neuronal line, Appl, with higher expression in neurons of the central brain (**Fig. 2B**). Next, we examined excitatory neurotransmitter subtypes. We again overexpressed the PPP1R15 phosphatase, now in select neuronal subpopulations, and examined alterations to distance traveled (**Fig. 2**), tissue eIF2α-P levels (**Supplemental Figure 1**), and survival (**Table 1**). We found decreased distance traveled when expressing PPP1R15 in glutamatergic and dopaminergic neurons (**Fig. 2C**) but not in other neurotransmitter subtypes.

We attempted to localize the phenotype to neuronal populations hypothesized to be important for regulating motor function in dystonia. We found that the distance traveled

increased relative to controls when we expressed PPP1R15 in either D1- or D2-type dopamine receptor neurons (**Fig. 2D-E).** (Martin et al., 1998). Notably, overexpressing PEK in fly dopaminergic neurons decreases distance traveled in locomotor assays (Elvira et al., 2020) and knocking down PEK in mouse dopaminergic neurons increases distance traveled, time moving, and number of steps in exploration and motor tasks (Longo et al., 2021), suggesting decreased eIF2α-P enhances dopamine signaling and locomotor drive.

Surprisingly, we also detected a phenotype when expressing PPP1R15 in a pan-glial driver (**Fig. 2F**), indicating that the motor phenotype may not exclusively map to neurons. We found no change in locomotor function when expressed in inhibitory (**Fig. 2G**) or central cholinergic excitatory neuron populations (**Fig. 2H**), although we did observe a stronger response to the tap stimulus when expressing PPP1R15+ in cholinergic neurons. We did not see a locomotor phenotype when PPP1R15 was overexpressed in motor neurons (**Fig. 2I**) or in the mushroom body (**Fig. 2J**), a higher-order brain structure important for initiating and ceasing movements

Increased eIF2α-P across the nervous system creates developmental lethality and locomotor impairments localizing to D2-expressing neurons

Given that we found that overexpression of PEK-kinase in neurons with the ELAV driver caused locomotor impairments (**Fig. 1E**), we examined the same battery of Gal4-driven neuronal lines and found overexpression of PEK in most lines caused early developmental lethality (**Table 2**). The requirement for PPP1R15 and PEK during development has been described previously (Malzer et al., 2010; Malzer *et al.*, 2013), but this demonstrates sensitivity to overexpression of PEK in multiple neuronal subpopulations. Interestingly, female Dop2R-PEK+ progeny survived and had decreased distance traveled in a locomotor assay (**Fig. 2M**) compared to increased distance in Dop2R-PPP+ (**Fig. 2E**). This is the only bidirectional phenotype observed in these studies, demonstrating an inverse relationship between eIF2α-P and locomotor drive, specifically in D2-receptor expressing neurons.

The Dop2R-Gal4 and Appl-Gal4 insertions are located on the female sex chromosome and are expressed twice as much in males compared to females. These 2 lines had female progeny surviving to adulthood, but males failed to survive. Therefore, PEK overexpression phenotypes are dose-dependent and not due to dominant effects of the P-element insertion.

Pan-neuronal and D2- neuronal alterations to eIF2α-P increase hyperkinetic movements in response to heat

Human dystonia can be precipitated by sensory stimuli such as heat (Pohl et al., 2002) or mechanosensory sensation, positive or negative emotion, or passive or volitional movement (Balint *et al.*, 2018). Dystonia-like movements manifest in flies with mutations in orthologs of dystonia genes *ATP1A3* and *DYT1* as hypokinetic or hyperkinetic repetitive movements evoked by mechanical and/or thermal stimulation (Ashmore et al., 2009; Koh *et al.*, 2004). This is thought to be due to increased heat increasing synaptic transmission and excitatory neuronal drive due to flies being a poikilothermic model (Peng et al., 2007). Dopamine-deficient states can lead to dystonia; tyrosine hydroxylase and GTP cyclohydrolase deficiency can lead to dystonia and treatment with L-Dopa can reduce dystonia (Calabresi and Standaert, 2019). We thus followed up our findings of bidirectional sensitivity to D2-driven PEK expression, where we observed a bidirectional sensitivity to eIF2α-P levels, hypothesizing that D2-specific increases in eIF2α-P might manifest with features of dystonia.

We captured videos over 3 minutes at 38˚C, a physiological temperature below the threshold to induce heat shock or paralysis from action potential propagation failure (Reenan and Rogina, 2008). We observed hyperkinetic movements in flies subjected to elevated temperatures that manifested as wing flapping in the absence of flight that were not present in either genetic control. Events where animals had wings in motion for >4 video frames while standing or walking were quantified. 82% (290/352) of bouts were 1 second or shorter. These bouts were present in animals expressing PEK+ in D2-receptor cells at a rate of 7.6 events/fly on average (**Fig. 3A**). Since these movements were not present in controls, we conclude that this was not an attempt at cooling.

Elevations in temperature also increase the number of fly movements, measured as flights, jumps, or drops (from the petri dish wall or ceiling). The frequency increases and then plateaus over time, consistent with heat-driven increase in activity followed by acclimation (**Fig. 3B**). The number of movements increased equally across all genotypes (**Fig. 3C**). However, Drosophila overexpressing PEK in D2 receptor neurons had abnormal movements (dyskinesias), operationally defined as difficulties in coordinating landings where an animal landed on its back, side, or abdomen instead of feet (**Fig. 3D**). We observed a 3-fold increase in abnormal landings during genotype-blinded scoring in flies with D2-neuronal elevated eIF2α-P compared to their genetic controls (**Fig. 3E**). Often, flies landing on their back or side had difficulty righting as well and required several attempts to return to standing (**Supplemental Video 1**). We identified good agreement between independent observers (Gwet AC1 95% CI 0.87-0.91, $p<10^{-16}$) in identifying these abnormal landings (dyskinesias).

Reduced eIF2α-P or overexpression of the htorΔE dystonia risk allele in cholinergic neurons increases hyperkinetic responses to mechanosensory stimulation with potential roles in reducing neurotransmitter release

We hypothesized that reductions in eIF2α-P may be altering neuronal or circuit properties to such as neurotransmission. Mechanical stimulation has previously been used to evoke hyperkinetic movements in Drosophila dystonia models (Ashmore *et al.*, 2009). We examined overexpression of the eIF2α phosphatase, PPP1R15+, in cholinergic neurons because of the observed sensitivity to mechanical tap stimulus in the locomotor assay. To determine sensitivity to a mechanosensory stimulus, flies were vortexed for 10 seconds and time to recover was recorded. We found that ChAT/PPP+ flies had increased duration of hyperkinetic movements, such as wing flapping without flight, and unsuccessful/dyskinetic movements, such as repeated attempts to stand after mechanical stimulation (**Fig. 4A**) although the total proportion of animals exhibiting dyskinetic movements did not change from ChAT/+ controls (**Fig. 4A'**). We hypothesized that similar dyskinetic movements may be present in a model of primary genetic dystonia and expressed the human *DYT1* risk allele, which featuring a deletion of glutamic acid at position 302/303 (htorΔE). We asked whether overexpression of the htorΔE dystonia risk allele in cholinergic neurons similarly increased sensitivity to a mechanical stimulus. Like flies overexpressing PPP1R15+, htorΔE flies had hyperkinetic and dyskinetic movements with mechanical stimulation, with longer time to recover (**Fig. 4B**) without changing the proportion of animals exhibiting dyskinetic movements (**Fig. 4B'**). In comparison, overexpressing wildtype human torsin A (htorA) as a control did not alter time to recover compared to control animals (**Fig. 4C**) or the number of flies exhibiting dyskinetic movements (**Fig. 4C'**).

Cell-intrinsic expression of htorΔE has been demonstrated to reduce dopamine neurotransmitter levels in a mouse model (Downs et al., 2021). To determine if the mechanosensitivity phenotype could be due to altered neurotransmission, we expressed a temperature sensitive mutant dynamin (*shibire*$^{ts-1}$) in cholinergic neurons to reduce neurotransmission. Flies were reared at low temperature (18˚C) and moved to room temperature for recording (22˚C) but kept below the restrictive temperature which induces paralysis (30˚C) (Kitamoto, 2001). We found reducing cholinergic neurotransmission also generated hyperkinetic and dyskinetic movements in response to mechanical stimulus, with longer time to recover (**Fig. 4D**) without changes in proportion of responders (**Fig.4D'**). These animals demonstrated a more extreme phenotype with infrequent, temporary paralysis thought to be due to increased muscle activation because paralysis was both proceeded and followed

by hyperkinetic movements. No paralysis or hyperkinetic movements were observed at room temperature in the absence of the mechanical stimulus (not shown). These results show that decreased eIF2α phosphorylation, htorΔE expression, and decreased neurotransmission in cholinergic neurons increase sensitivity to mechanically elicited dystonia-like movements.

Increased eIF2α-P increases axon terminal size

Since eIF2α-P modifications induce heat- (**Fig. 3**) and mechanosensory-evoked (**Fig. 4**) hyperkinetic and dyskinetic movements and increased eIF2α-P has been observed to decrease dendrite arbor size (Tsuyama et al., 2017), we asked if eIF2α-P levels regulate synaptic connectivity. Regulation of connectivity could be mediated through eIF2α-P inhibition of protein translation, which is required for both LTP and LTD long-term neuron plasticity, or gene expression downstream of ATF4. Increased connections between brain regions have been identified in dystonia patients (Niethammer *et al.*, 2011 ; Vo *et al.*, 2015). Further, alterations to synaptic plasticity have been observed including a decreased threshold for LTP and absent LTD in a htorΔE mouse model (Maltese *et al.*, 2018) and impaired LTD with intact LTP in *DYT6* mouse models (Zakirova *et al.*, 2018). Finally, reduced dopamine release has been observed in an *ATP1A3* shRNA knockdown mouse model (Fremont et al., 2015) suggesting that synaptic release and connectivity may be altered in dystonia. To determine if alterations in synaptic connectivity occurred with genetic manipulation of eIF2α-P levels, we examined the neuromuscular junction using immunostaining (**Fig. 5A-B**). We assessed a whole-animal, partial loss of function (LoF) of *PPP1R15* with confirmed increases in eIF2α phosphorylation. We found increased axon terminal size relative to muscle area in PPP1R15$^{-/-}$ homozygotes (**Fig. 5C**). This suggests increases in synaptic connectivity may arise from alterations to eIF2α phosphorylation and could potentially underlie changes to motor control, although whether this was due to impaired LTD or other mechanisms is unclear.

Pharmacologic bypass of eIF2α-P protein synthesis suppression does not rescue locomotor phenotypes

We investigated whether bypassing the translational suppression caused by elevated eIF2α-P could improve outcomes in our model. We utilized ISRIB, a compound that activates eIF2B and permits protein synthesis despite eIF2α-P status (Zyryanova et al., 2021). We overexpressed PEK in central brain neurons with the Appl driver and treated animals with either ISRIB or vehicle control during larval development. We first determined that there was no developmental or early adult lethality (not shown) or change in distance traveled in genetic

controls treated with vehicle or 500 nM ISRIB treatment (**Fig. 6A**). We then studied locomotor ability in adults and survival in Appl-PEK+ animals when treated with ISRIB. We did not detect a difference in distance traveled between vehicle-treated controls and ISRIB-treated Appl-PEK+ expressing animals (**Fig. 6B**). However, we did observe that treatment with ISRIB during development significantly improved adult lifespan (**Fig. 6C**). This suggests that disrupted global protein translation secondary to elevated eIF2α-P may be contribute to adult survival, but other factors, such as ATF4 signaling (**Fig. 1F**) may be contributing to locomotor dysfunction in our dystonia model of elevated eIF2α-P.

Discussion

The regulation of the eIF2α phosphorylation is tightly controlled, with dysregulation emerging as a candidate mechanism for dystonia of diverse origins. In these studies, we investigated whether disrupting eIF2α-P signaling alone would be sufficient to elicit motor features of dystonia using a Drosophila model. Consistent with this, we found eIF2α-P is required for development of normal motor function in both glia and neurons, with further localization to cholinergic, dopaminergic/glutamatergic, and dopamine-receptor expressing neurons. Increased eIF2α-P in D2-receptor expressing neurons and decreased eIF2α-P in cholinergic neurons increases susceptibility to hyperkinetic and dyskinetic movements in the presence of heat and mechanical stimulation, respectively. We identified overlap between a cholinergic cell type origin of mechanosensitivity with an independent dystonia model, the ΔE allele of torsin/*DYT1* (Koh *et al.*, 2004; Wakabayashi-Ito et al., 2015). Mechanosensitivity was also achieved with suppressed neurotransmission using a dynamin mutant; interestingly, variants in *DYN1* have also been identified as a genetic cause of dystonia (von Spiczak et al., 2017). We identified increased synaptic terminal size from a PPP1R15 partial LoF variant that increased eIF2α-P. Together, these results suggest either increased or decreased eIF2α-P can increase sensitivity to evoked hyperkinetic/dyskinetic movements, likely through disrupted dopamine and acetylcholine signaling which may increase synaptic connectivity in the long-term. Our data suggests that the directionality of the eIF2α-P effect is likely cell-type dependent.

These findings suggest elevated eIF2α-P within D2-expressing neurons fails to suppress abnormal movements when excitatory drive is high. Activation of D2 receptors expressed within the mammalian indirect pathway act as a brake for unwanted movements, and the loss of this suppression has been identified in various hyperkinetic movement disorders (Calabresi and Standaert, 2019). Although an indirect motor pathway has not been described in Drosophila, D2

receptor activation inhibits neuronal activity across both species and D1 receptor binding activates a direct pathway that drives motor activity and arousal in the central complex, a structure homologous to the vertebrate basal ganglia. (Karam et al., 2020). We observed increased locomotor activity with decreased eIF2α-P in both D1- and D2-receptor expressing neurons, suggesting D2-type neurons may normally inhibit movement in flies and D1 neurons may normally drive movements (**Fig. 2D-E**). Activation of D1 receptors while suppressing of D2-receptors subsequently increasing motor drive has been observed in focal dystonias (Simonyan et al., 2017). Consistent with our finding that both D1- and D2-receptor expressing neurons are sensitive to eIF2α-P perturbations, overexpressing PEK specifically in dopaminergic neurons reduces distance traveled in a locomotor assay in older Drosophila and those subjected to chronic heat stress (Elvira *et al.*, 2020). We further observed that D2 neurons are important for suppressing dyskinetic and hyperkinetic movements with heat stimulation (**Fig. 3**). Together this demonstrates that eIF2α-P dysregulation in both dopamine releasing neurons and neurons modulated by dopamine, especially D2-receptors, can lead to alterations in motor control.

We also found increased sensitivity to mechanical stress, but only in the cholinergic neurons. In vertebrates, alterations to acetylcholine in the striatum regulating dopamine release is a candidate for dystonia pathophysiology (Eskow Jaunarajs *et al.*, 2015). In insects, acetylcholine is a central excitatory neurotransmitter. In both vertebrates and insects, acetylcholine plays an important role in inhibitory control for suppressing movements (Sabandal et al., 2022). One possible mechanism is acetylcholine activation of mAChRs facilitates dopamine release in the striatum (Lester et al., 2010) and D2 receptors play a key role in motor inhibition, with abnormal D2 signaling contributing to both tardive dyskinesias and dystonia (Calabresi and Standaert, 2019). We found evoked hyperkinetic and uncoordinated movements when we decreased eIF2α-P levels in cholinergic neurons and increased eIF2α-P levels in D2-receptor neurons. Acetylcholine is predicted to increase release of dopamine, inhibiting neurons expressing D2 receptors. This suggests a model where decreased neurotransmission, such as through decreased eIF2α-P, in cholinergic neurons or decreased responsiveness, such as through increased eIF2α-P, in D2-receptor expressing neurons can uncover dystonia-like hyperkinetic movements or other motor impairments.

Studies of the motor circuit in dystonic patients have identified altered connectivity between sensory-motor cortex, thalamus, cerebellum, and basal ganglia (Vo et al., 2015; Niethammer et al., 2011). It is hypothesized that disrupted synaptic plasticity, connectivity, neurotransmission, or neuromodulation may underlie the circuit changes. Heat and mechanical stimulation in Drosophila increase global neuronal activity and likely represent increased excitatory drive onto

sensitized cell types, resulting in hyperkinetic motor activity. Therefore, the molecular changes from either increased or decreased eIF2α-P and htorΔE may be reducing the release of neurotransmitters that inhibit unwanted movements or abnormally increased synaptic connectivity. Consistent with this, both decreased calcium transients (Beauvais et al., 2016) and enhanced LTP (Maltese *et al.*, 2018) have been observed in DYT1 models.

Phosphorylation of eIF2α is a key step in translation-dependent synaptic plasticity. Reducing eIF2α-P by knocking out PEK or GCN2 or expressing a nonphosphorylatable eIF2α allows induction of LTP with less strict stimulation protocols (Chesnokova *et al.*, 2017; Costa-Mattioli et al., 2005; Longo *et al.*, 2021). LTD requires phosphorylation of eIF2α-P to express uORF-regulated mRNA that regulate AMPA receptor endocytosis. Notably, eIF2α-P induction of LTD occurs in the absence of cellular stress (Biever et al., 2016; Di Prisco et al., 2014). Our findings suggest that eIF2α-P defects may generate alterations to cellular and synaptic properties that impair motor control in a cell-specific manner. We also identified phenotypic overlap between decreasing eIF2α-P, expressing htorΔE, and decreasing neurotransmitter release in cholinergic neurons. In contrast, decreased eIF2α-P in dopaminergic neurons seemingly increases neurotransmitter release and uptake, enhanced LTD and LTP, and increased motor activity (Longo *et al.*, 2021). Our findings suggest decreased eIF2α-P may suppress dopamine and/or acetylcholine while elevated eIF2α-P in D2-receptor neurons may increase synaptic connectivity and both can generate dystonia-like movements in our model.

We identified the overexpression of ATF4, a transcription factor translated with elevated eIF2α-P signaling, was also sufficient to generate motor impairments in a locomotor assay. ER stress from misfolded proteins (Alharbi et al., 2023) regulators of eIF2α-P such as PRKRA (Zech *et al.*, 2014), and downstream factions including ATF4 (Rittiner *et al.*, 2016) are being identified as individual genetic causes of dystonia. Consistent with this, we found restoring protein translation with ISRIB did not improve locomotor function with elevated eIF2α-P, suggesting ATF4 or other eIF2α-P specific translation could play an important role in these locomotor impairments. It remains unknown what differences in uORF-regulated genes could be abnormally regulated in dystonia, what impact those factors have on synaptic/neuronal plasticity, and whether they would be a potential target for treatments.

Acknowledgements

We are grateful to Nahla Haque, Megan Kotzin, James Liu, Rosario Padilla Sánchez, Andrew Musmacker, Frances Nowlen, Tristan Shackelford, Zach Tiede, and Bryce Wilson for

assistance with Drosophila rearing, assays, and western blotting. We are also grateful to Daniela Zarnescu and Robert Kraft for advice and training.

We are grateful to Naoto Ito for the kind gift of htor fly stocks and FlyORF for ATF+ and PPP+. The remaining stocks were obtained from the Bloomington Drosophila Stock Center (NIH P40OD018537). The monoclonal antibody developed by C. Goodman was obtained from the Developmental Studies Hybridoma Bank, created by the NICHD of the NIH and maintained at The University of Iowa, Department of Biology, Iowa City, IA 52242. Biomedical Imaging Core microscopy facilities at the University of Arizona College of Medicine – Phoenix were used in these studies.

SL is supported by the CPARF PRG06621 and MCK is supported by funding from NIH (1R01NS106298 and 1R01NS127108).

Declaration of Competing Interests

The authors declare no competing interests.

Author contributions

Conceptualization, S.A.L., M.C.K; Methodology, S.A.L.; Investigation, S.A.L., J.F., J.T.; Writing—original, S.A.L; Writing-Review & Editing, S.A.L., S.P.L, M.C.K.; Funding Acquisition, S.A.L., M.C.K.

Figures and Tables

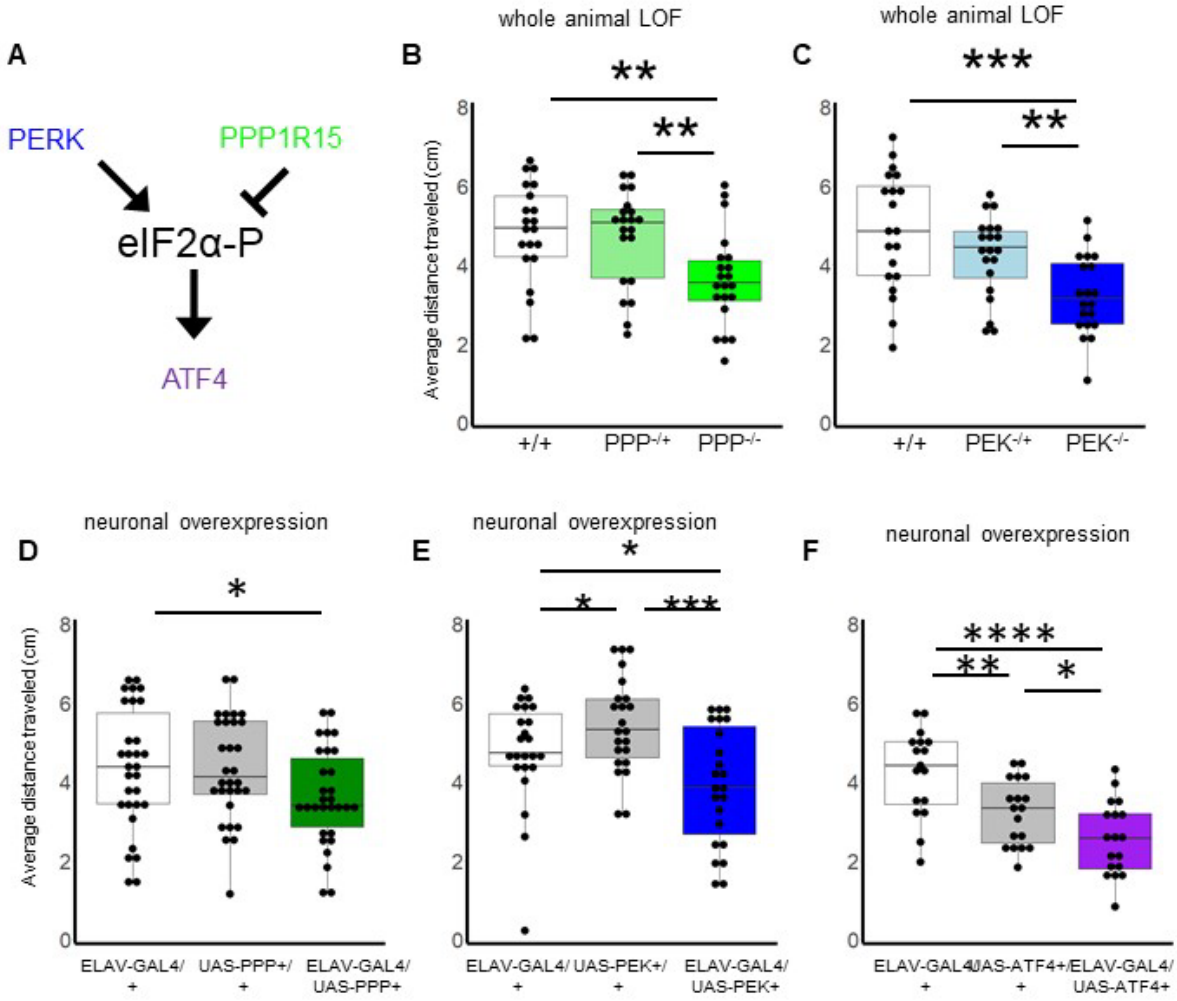

Fig. 1 Regulation of eIF2a-P and ATF4 is required for locomotor ability in the fly nervous system. A. Schematic diagram showing regulation of eIF2α phosphorylation (eIF2α-P) by PERK (PEK) kinase and negative regulation by PPP1R15 (PPP) phosphatase. B-F. Quantification of distance traveled in negative geotaxis assay after 3 seconds. Whole animal loss-of-function variants in PPP (B) and PEK (C) have locomotor impairments. Overexpression of PPP (D) and PEK (E) in neurons using an ELAV-Gal4 driver also causes locomotor impairments. F. Overexpression of ATF4 also causes locomotor impairments, demonstrating ATF4 expression of stress response or plasticity genes may be mediating the changes to locomotor function.

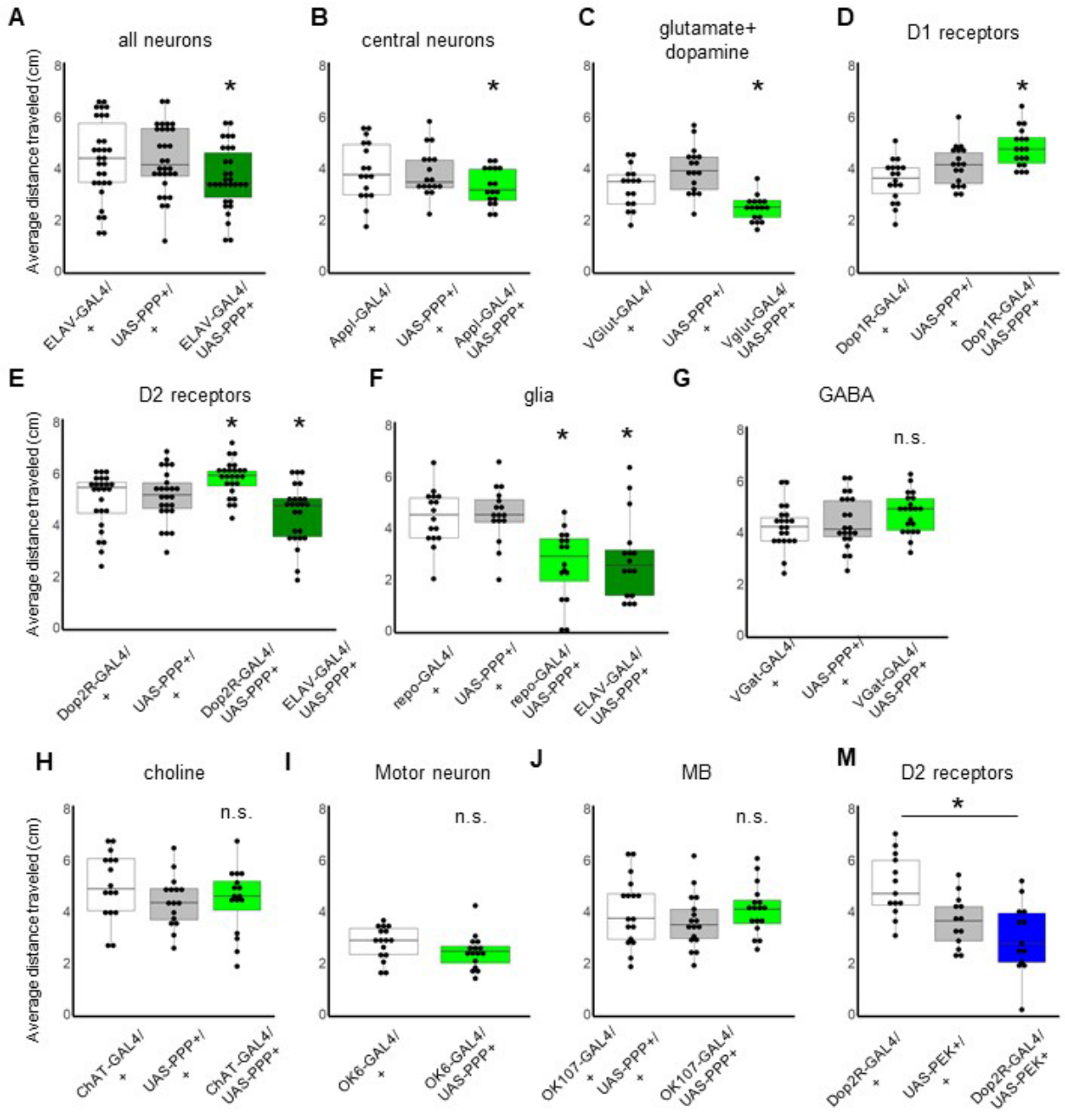

Fig. 2 Mapping requirement for eIF2α-P in specific cell types using PPP+ or PEK+ overexpression. A-J. Quantification of distance traveled in flies overexpressing PPP+ (green). Overexpressing PPP in all neurons (A, also Fig. 1D), central brain neurons (B), and glutamatergic and dopaminergic neurons (C) decreases locomotor function. Overexpressing PPP+ in neurons expressing dopamine receptors D1 (D) and D2 (E) increased distance traveled. Glial expression (F) was also found to impair locomotor function. There was no change in locomotion with expression in inhibitory GABA (G), excitatory cholinergic (H), glutamatergic motor (I) or mushroom body (J) neurons. M. Quantification of distance traveled in flies overexpressing PEK+ (blue) in D2-type expressing neurons. Overexpressing PEK+ decreased distance traveled. MB=mushroom body lobes. * $p<0.05$ by paired 2-tailed t-test for both controls unless specified with a bar. Statistic details in Table 1 and 2.

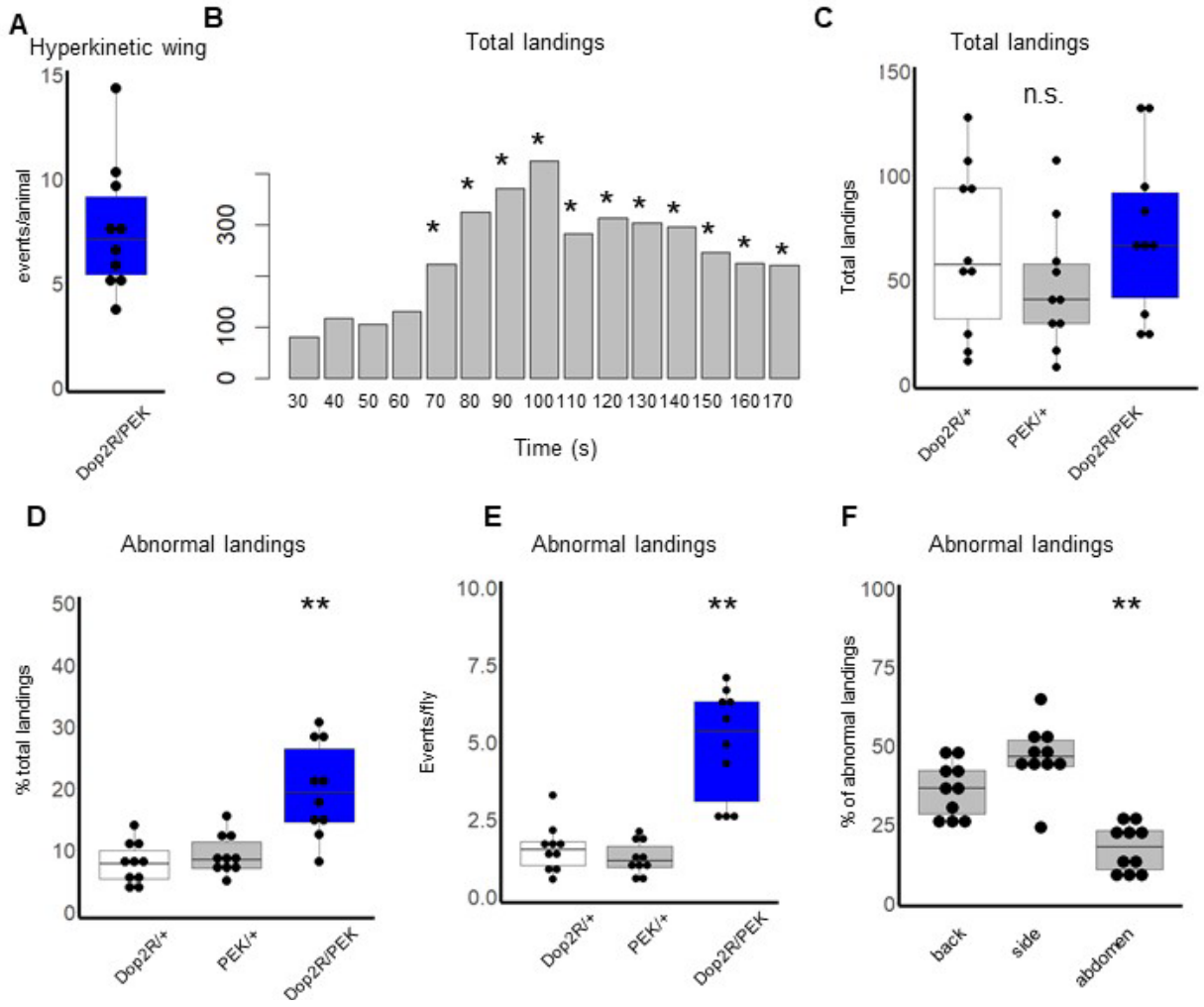

Fig. 3 Heat-sensitive movements from elevated eIF2α-P in D2 neurons. A. Hyperkinetic wing events per animal, defined as flapping in the absence of flight, were only observed in Dop2R/PEK flies. B. The number of flights and jumps increases significantly with exposure to 40˚C temperature. C. There is no difference in total movements between genotypes. D-E. The proportion of abnormal landings per total landings (D) and per fly (E) was significantly increased in Dop2R/PEK flies. F. Distribution of the body part of the flies involved in abnormal landings. The back and side of the animal contacted the floor significantly more often than the abdomen. Statistics: B, 10 trials, 3663 landings, D2-PEK only, * $p<0.05$ t-test vs at baseline measured between 30-40 seconds after starting video. D-E, ** $p<0.001$ t-test between both Dop2R/+ and PEK/+ control and Dop2R/PEK. F, 10 trials, 628 total abnormal landings, D2-PEK only, ** $p<0.001$ t-test compared to both side and back.

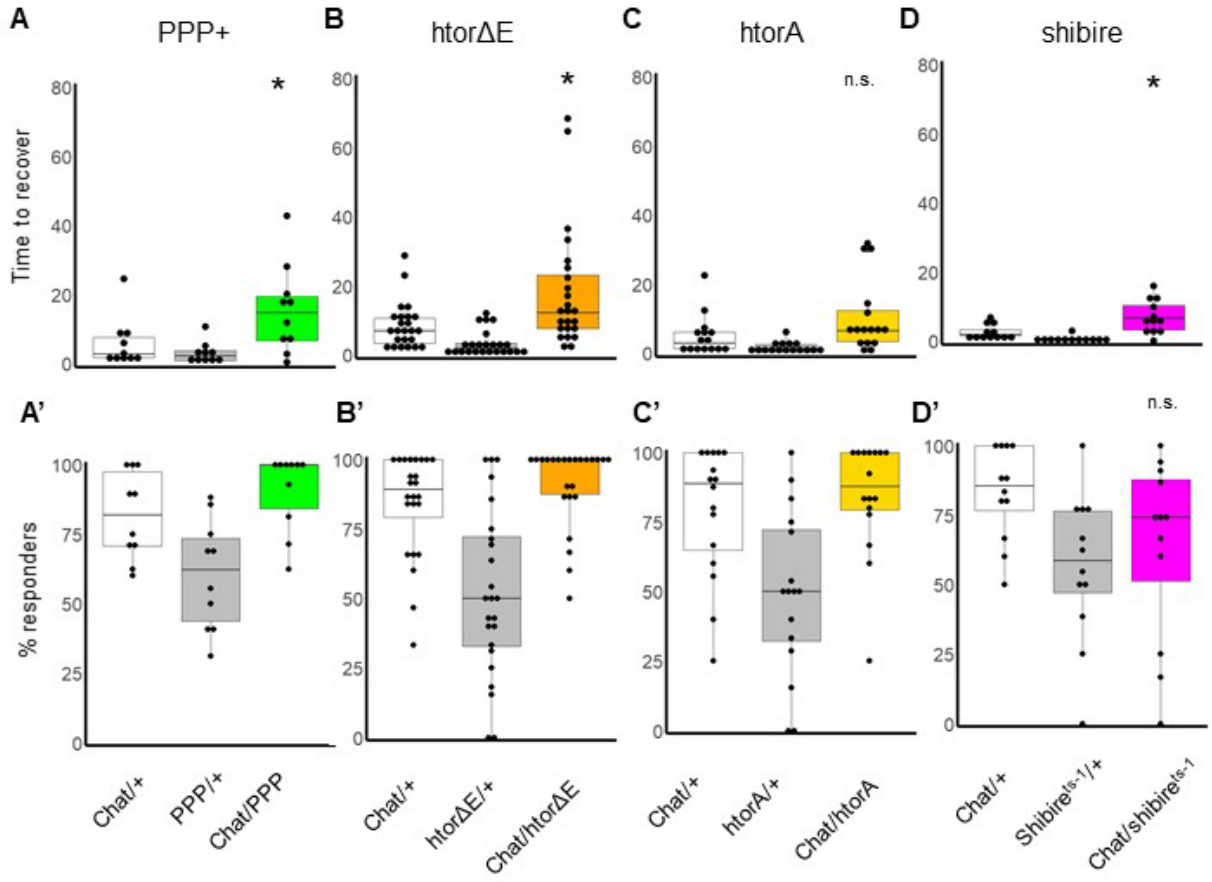

Fig. 4 Sensitivity to mechanical stimulation with cholinergic expression of PPP1R15+ and htorΔE dystonia models and neurotransmission silencing. A-D, Quantification of recovery time. Expression of PPP1R15+ (A) and htorE (B) in cholinergic excitatory neurons increases time to recover from a mechanosensory event compared to controls. In contrast, expressing control htorA (C) does not change recovery compared to controls. Expressing temperature sensitive dynamin (shibirets-1) in cholinergic neurons also increases the time to recover from mechanical stimulation (D). A'-D', Quantification of percent of animals responsive to mechanosensory stimulus. There is no difference in the proportion of flies responding to the mechanical stimulus when compared to both heterozygous controls. * p≤ 0.05, paired 2-tailed t-test, average 9 flies/trial.

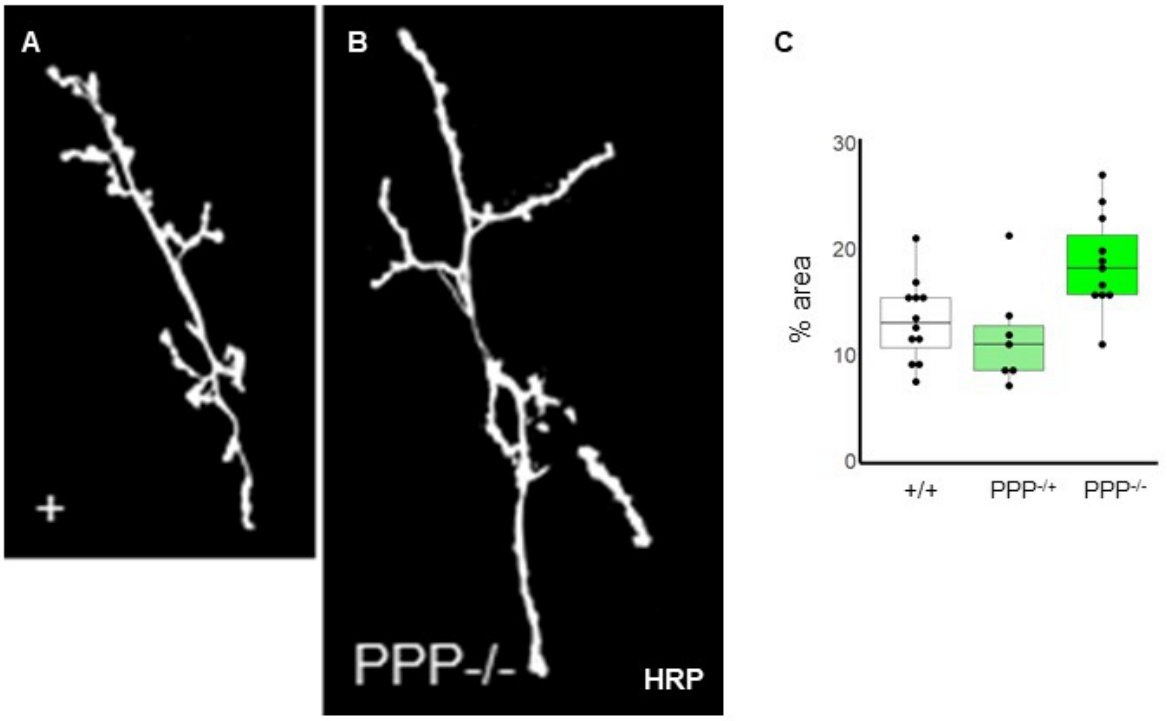

Fig. 5 Increased eIF2α-P by reductions in PPP1R15 expression increases axon terminal size at the neuromuscular junction. A-B Sample images reconstructed from confocal stacks with neuron membrane visualized by anti-HRP used for quantification. A, genetic control. B, *PPP1R15*^{G18907} homozygote. C, quantification of the neuron area (HRP) normalized to 100 μm^2 muscle area.

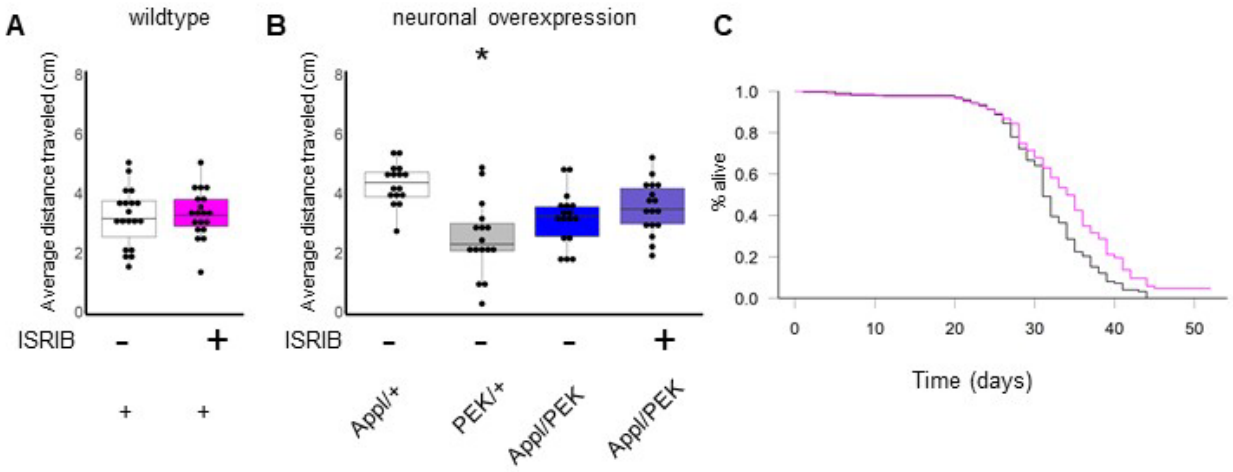

Fig. 6 Pharmacological modification of developmental protein translation improves survival from elevated eIF2α-P, but not locomotor function. A-B Distance traveled with ISRIB treatment to bypass eIF2α-P suppression of protein translation. A. There was no change in distance traveled in CantonS wildtype (A) or Appl-PEK+ (B) animals following treatment with ISRIB. C. survival curve examining the proportion of alive flies over time in days. C. Survival of Appl-PEK animals receiving 500 nM ISRIB (magenta) during development is significantly improved compared to animals receiving 0.25% DMSO solvent control alone (black). Chi square p= 7e-05. ISRIB: n=18. T test App vs App/PEK DMSO 0.0003 T test PEK vs App/PEK DMSO) n.s. 0.08 T test DMSO v ISRIB n.s. 0.27

	line name	Expression	Vial	Change to eIF2α-P (WB)	Other phenotypes
Whole animal	PEK-	whole animal	Decreased distance (n=21)	Decreased (n=4 bio, 2 tech)	NMJ increased
Neuronal	ELAV	post mitotic neurons	Decreased distance (n=30)	Decreased (n=4 bio, 2 tech)	
	Appl	neurons, central brain> VNC>salivary glands+fat body. higher in males. Larva-adult.	Decreased distance (n=17)	Decreased (n=4 bio, 3 tech)	
Inhibitory	VGAT	GABA vesicle transport; inhibitory interneurons	No difference (n=22)	Decreased (n=3 bio, 3 tech)	
Excitatory	ChAT	choline acetyltransferase; excitatory neurons	No difference (n=16)	Decreased (n=4 bio, 4 tech)	Mechanical sensitivity (n=24)
	VGlut	glutamatergic and dopaminergic neurons	Decreased distance (n=17)	No difference (n=5 bio, 3 tech)	
Dopamine receptors	Dop2R	dopamine receptor GPCR; nervous, digestive, excretory systems	Increased distance (n=25)	Decreased (n=4 bio, 3 tech, females)	
	Dop1R	dopamine receptor GPCR; gamma Kenyon cell, adult MB, optic lobe	Increased distance (n=19)	SL324 (4 bio replicates, 3 tech) n.s. vs. Dop1R/+ decreased vs. PPP/+	
Glial	Repo	glia	Decreased distance (n=16)	Trend toward decreased, but n.s. (4 bio, 3 tech)	Pupal and early adult lethality; males more affected.
Specific subtypes	OK6	motor neurons (glutamatergic)	No difference (n=16)	Not tested	
	OK107	Mushroom body neurons + neuroblasts	No difference (n=17)	Not tested	

Table 1: Behavioral and molecular phenotypes from reduced eIF2α-P due to PEK partial LoF or PPP151R overexpression. Information about lines used for driving cell-specific expression can be found in **Supplemental Table 1**.

Biological replicates for western blotting indicate mixed batches of 20-40 adult heads, technical replicates indicate the same samples run on different blots.

	Gal4 name	Localization	Vial	Change to eIF2α-P (WB)	Other phenotypes
Whole animal	PPP-	whole animal	Decreased (n=20)	Increased (4 bio, 2 tech)	Increased NMJ size
Neuronal	ELAV	post mitotic neurons	Decreased distance (n=23)	Increased (4 bio, 4 tech)	
	Appl	neurons, central brain> VNC>salivary glands+fat body. higher in males. Larva-adult.	Decreased distance (n=15)	Increased (n=4 bio, 3 tech)	Males dead
Inhibitory	VGAT	GABA vesicle transport; inhibitory interneurons	Dead	Dead	
Excitatory	ChAT	choline acetyltransferase; excitatory neurons	Dead	Dead	
	VGlut	glutamatergic and dopaminergic neurons	Dead	Dead	
Dopamine receptors	Dop2R	dopamine receptor GPCR; nervous, digestive, excretory systems	Decreased distance (n=13)	Increased (n=6 bio, 4 tech, females)	Hyperkinetic and dyskinetic in heat assay (n=10) males dead
	Dop1R	dopamine receptor GPCR; gamma Kenyon cell, adult MB, optic lobe	Dead	Dead	
Glial	repo	glia	Dead	Dead	
Specific subtypes	OK6	motor neurons (glutamatergic)	Dead	Dead	
	OK107	Mushroom body neurons + neuroblasts	Dead	Dead	

Table 2. Behavioral and molecular phenotypes from increased eIF2α-P due to PPP partial LoF or PEK overexpression. Information about lines used for driving cell-specific expression can be found in **Supplemental Table 1**.

Biological replicates for western blotting indicate mixed batches of 20-40 adult heads, technical replicates indicate the same samples run on different blots.

Methods

Drosophila genetics and rearing

Drosophila reared on a standard cornmeal, yeast, sucrose food from the BIO5 media facility, University of Arizona. Stocks for experiments reared at 25°C, 60-80% relative humidity with 12:12 light/dark cycle. Cultures for controls and mutants were maintained with the same growth conditions, especially the density of animals within the vial. The GAL4-UAS system was used to drive cell-type specific expression of eIF2α-P genetic modulators (Caygill and Brand, 2016). For experiments using whole-animal partial loss of function alleles, controls were *yw* homozygotes and heterozygotes from the cross between *yw* and the loss-of-function homozygous stock. For Gal4-UAS experiments, controls were heterozygotes from the Gal4 and UAS lines crossed with w^{1118}.

w^{1118}, *yw*, and Canton(S) were acquired from Bloomington Stock center (NIH P0OD018537). w^{1118} was outcrossed with Canton-S and backcrossed with w^{1118} for 12 generations while selecting for red eyes. UAS-crc (ATF4+) was acquired from FlyORF (Bischof et al., 2013). The creation of htorΔE and htorA described in (Wakabayashi-Ito *et al.*, 2015) and were a kind gift from Naoto Ito.

A complete list of genotypes, source, and expression information can be found in **Supplemental Table 1**.

Western blotting and quantification

Protein samples prepared from heads of 10-20 males and females in protein extraction buffer plus 1% protease inhibitor (ThermoFisher) and 1% phosphatase inhibitor (Sigma) as previously described (Emery, 2007). Western blotting performed according to standard methods with detection on a 0.2 μm nitrocellulose membrane. For eIF2α, phosphorylation antibody was imaged first, then the membrane was washed and reprobed for total eIF2α. Antibodies used for study are listed in **Supplemental Table 2**. eIF2α-P: 1:1000 rabbit α phospho-S51 (Cell Signaling 3597), 1:500 rabbit α eIF2S1 (Abcam 4837) and detected with a 1:10000 goat anti rabbit secondary antibody conjugated with HRP and imaged with ECL (GE healthcare NA931, NA934).

Chemoluminescence captured using FluorChem Imager (Biotechne) and quantified with Image studio Lite (LiCor). eIF2α phosphorylated/total ratio was normalized to Gal4/+ heterozygous control for each biological replicate. The same size area was used to measure total protein and puromycin signal for each lane to reduce variability. Four independent

biological samples were collected for quantification; different blots or lanes of the same samples indicated as technical replicates. Differences between genotypes calculated using 2-tailed paired t-test statistic and graphs generated using R (4.2.2). Software packages used to analyze data can be found in **Supplemental Table 3**.

Drosophila movement assays

We used naïve, unmated flies collected as pharate adults and sequestered for 14 days before recording. Flies were adapted to room conditions for 1 hour before moving to empty assay tubes or petri dishes in groups of 10-20. All assays included sex-matched genetic controls as part of the trial. Flies of both sexes were used for all experiments except for Dop2R-PEK and Appl-PEK due to male lethality. Video recorded with Canon EOS Rebel T7 camera and visualized with Premier Pro or Rush (Adobe).

Distance traveled assay was performed using paired, coded vials of control and mutant flies (Kim et al., 2016). Distance measured from still image from video at 3 seconds post-tapping using ImageJ (NIH, v.1.50i) to measure distance function from middle of fly to bottom of vial for 12-30 trials.

The adult heat assay was adapted from (Koh *et al.*, 2004) with scoring of the video to quantify hyperkinetic and uncoordinated movements. Groups of flies were loaded via aspirator into 3 cm petri dishes, matched for number of flies and sex for each recording. Damp filter paper was used to regulate humidity in heat assay chamber. Temperature was regulated by water bath with 37˚C temperature continuously monitored. Video recorded for 3 minutes after assay chamber submersion. Hyperkinetic wing events were defined as wings in motion for >4 video frames during a non-flight behavior such as walking or standing; flies landing or initiating flight afterwards were excluded. Videos were scored for the number of total floor landings (defined as any action where a fly contacted the floor, such as after a drop, flight, or jump from any surface of the petri dish. Abnormal landings were defined as when the fly contacted the floor with the caudal tip of the abdomen, side, or back. Abdomen landings required the fly to be perpendicular to the floor with no legs in contact. Side landings required the fly to have all six legs visible and more than 2 video frames to reach an upright position. Two independent scorers were used to develop criteria for scoring and for scoring Dop2R-PEK. Multiple iterations of training, feedback, and criteria clarification were used until >90% agreement was achieved for all 10 trials. Scorers were blind to genotype during scoring total and abnormal landings.

The adult mechanosensitivity assay was adapted from the method described previously (Ashmore *et al.*, 2009). Drosophila were collected as late-stage pupae and sequestered in standard food vials with 10-20 animals/vial and separated by sex. The animals were maintained

at 25°C, 30-60% relative humidity with 12:12 light/dark cycle. Groups of 10-20 at 14 days post eclosion were allowed to acclimate to the environment for one hour. The animals were then transferred to empty vials and subjected to intense mechanosensory disturbance for 10 seconds input via Vortex Genie 2 on the highest speed. Recordings were collected until all animals recovered. For scoring, each fly was observed, and the total time required to stand without restarting hyperkinetic movements. An animal was considered to be recovered after successful flight, walking up the side of the vial, or remaining stationary on its feet while grooming. Flies that did not respond to the stimulus were scored with a zero.

Graph creation and statistical test calculations were performed using R (4.2.2). For boxplots graphs, boxes represent 25th and 75th percentiles; whiskers represent 10th and 90th percentiles, and individual measurements are overplotted. Significance for average distance in vial assays determined using 2-tailed paired t-test. Difference in proportion of abnormal landings and hyperkinetic events calculated using 2-tailed unpaired t-test. The increase of total landings over time was calculated via 2-tailed unpaired t-test between baseline (30-40 seconds) versus other time bins. Gwet AC1 was used to test scorer agreement and to determine when a scorer had finished training using the R irrCAC package. For Gwet AC1 calculation, contingency tables were created between scorers across trials, using the number of all landings to identify agreement for a binary abnormal/normal classification.

Immunohistochemistry and imaging at the neuromuscular junction

Imaging of neuromuscular junction of 3rd instar wandering larva performed as previously described (Estes et al., 2011; Lewis *et al.*, 2023). Briefly, larval filet was dissected in HL-3 Ca++-free saline before fixation in Ca++ free 4% PFA. Washes performed with PBS with or without 0.1% Triton-X. Blocking before and during primary and secondary antibody steps using PBST with 5% normal goat serum, 2% BSA. Antibodies used in study listed in **Supplemental Table 2**. Primary antibody 1:400 M α DLG (4F3) incubated overnight at 4°C. DLG DSHB hybridoma monocolonal antibodies deposited by Goodman, C. Secondary antibodies 1:400 G α R Cy3 (ThermoFisher) incubated for 1.5 hours at RT. Neuronal membranes visualized with 1:100 Gα-HRP-Alexa 647 (Jackson ImmunoResearch) added with secondary antibody; HRP=horseradish peroxidase which recognizes neuronal membranes in Drosophila. 1:300 phallodin-488 in PBS (Molecular Probes) added as the final wash before mounting. Imaging performed with 710 Zeiss confocal using 1.0 µm Z-stack at 63x of the 1b 6/7 muscle in the A2 abdominal segment. Image parameters (laser gain and intensity, resolution, zoom) were kept constant between images of the same session, alternating between control and mutants.

Maximum intensity projections were created for a given field of view (FOV) using all parts of the Z-stack that included the axon terminal (defined by HRP staining) for all channels. Projections converted to greyscale from RGB in Photoshop (Adobe) without adjustments to pixel intensity. Non 6/7 1b HRP staining was identified based on shape/size/HRP staining intensity and manually removed.

Images analyzed using ImageJ software v. 1.50i (National Institutes of Health). Images from HRP channel converted to black and white using threshold feature with the threshold held uniform for images within an imaging session. NMJ area measured by drawing around area encompassed by both muscles and neuron in the FOV. Orthogonal projections converted to 8-bit black and white tiffs without thresholding. Boutons counted manually from 63x images stitched over entire neuron area. Statistics and graphs created using R (4.2.2) using the tidyverse library. For boxplots graphs, boxes represent 25^{th} and 75^{th} percentiles; whiskers represent 10^{th} and 90^{th} percentiles, and individual measurements are overplotted.

Treatment with ISRIB

We modified a previously described protocol for feeding ISRIB to developing larva (Ly et al., 2020). ISRIB was dissolved in a stock solution with DMSO and mixed with warmed fly food to a final concentration of 500 nM ISRIB and 0.25% bromophenol blue. Successful uptake of drug was confirmed by examining larval gut for bromophenol blue. Control animals were reared on an equivalent final concentration of DMSO (0.3%) and 0.25% bromophenol blue.
For survival, *Drosophila* were collected as late-stage pupae, separated by sex, and sequestered in standard food vials with ~20 animals/vial. The number of alive animals were monitored daily, with animals transferred to fresh food once per week. Survival library in R (4.2.2) was used to generate Kaplan-Meier plots and the log-rank test statistic.

Resource Availability Statements

This study did not generate new unique reagents or original code. All datasets available upon reasonable request.

References

Alharbi, H., Daniel, E.J.P., Thies, J., Chang, I., Goldner, D.L., Ng, B.G., Witters, P., Aqul, A., Velez-Bartolomei, F., Enns, G.M., et al. (2023). Fractionated plasma N-glycan profiling of novel cohort of ATP6AP1-CDG subjects identifies phenotypic association. J Inherit Metab Dis. 10.1002/jimd.12589.

Ashmore, L., Hrizo, S., Paul, S., Van Voorhies, W., Beitel, G., and Palladino, M. (2009). Novel mutations affecting the Na, K ATPase alpha model complex neurological diseases and implicate the sodium pump in increased longevity. Hum Gent *126*, 431-447.

Balint, B., Mencacci, N.E., Valente, E.M., Pisani, A., Rothwell, J., Jankovic, J., Vidailhet, M., and Bhatia, K.P. (2018). Dystonia. Nat Rev Dis Primers *4*, 25. 10.1038/s41572-018-0023-6.

Beauvais, G., Bode, N., Watson, J., Wen, H., Glenn, K., Kawano, H., Harata, N., Ehrlich, M., and Gonzalez-Alegre, P. (2016). Disruption of protein processing in the endoplasmic reticulum of DYT1 knockin-in mice implicates novel pathways in dystonia pathogenesis. J Neurosci *36*, 10245-10256.

Biever, A., Boubaker-Vitre, J., Cutando, L., Gracia-Rubio, I., Costa-Mattioli, M., Puighermanal, E., and Valjent, E. (2016). Repeated Exposure to D-Amphetamine Decreases Global Protein Synthesis and Regulates the Translation of a Subset of mRNAs in the Striatum. Front Mol Neurosci *9*, 165. 10.3389/fnmol.2016.00165.

Bischof, J., Björklund, M., Furger, E., Schertel, C., Taipale, J., and Basler, K. (2013). A versatile platform for creating a comprehensive UAS-ORFeome library in Drosophila. Development *140*, 2434-2442. 10.1242/dev.088757.

Calabresi, P., and Standaert, D.G. (2019). Dystonia and levodopa-induced dyskinesias in Parkinson's disease: Is there a connection? Neurobiology of disease *132*, 104579-104579. 10.1016/j.nbd.2019.104579.

Calvo, S.E., Pagliarini, D.J., and Mootha, V.K. (2009). Upstream open reading frames cause widespread reduction of protein expression and are polymorphic among humans. Proc Natl Acad Sci U S A *106*, 7507-7512. 10.1073/pnas.0810916106.

Caygill, E., and Brand, A. (2016). The GAL4 system: a versatile system for the manipulation and analysis of gene expression. Methods Mol Biol *1478*, 33-52.

Chesnokova, E., Bal, N., and Kolosov, P. (2017). Kinases of eIF2a switch translation of mRNA subset during neuronal plasticity. Int J Mol Sci *18*, E2213.

Chou, A., Krukowski, K., Jopson, T., Zhu, P., Costa-Mattioli, M., Walter, P., and Rosi, S. (2017). Inhibition of the integrated stress response reverses cognitive deficits after traumatic brain injury. Proc Natl Acad Sci U S A *114*, E6420-E6426.

Clemens, M.J. (2005). Translational control in virus-infected cells: models for cellular stress responses. Semin Cell Dev Biol *16*, 13-20. 10.1016/j.semcdb.2004.11.011.

Corona, C., Pasini, S., Liu, J., Amar, F., Greene, L.A., and Shelanski, M.L. (2018). Activating Transcription Factor 4 (ATF4) Regulates Neuronal Activity by Controlling GABA(B)R Trafficking. J Neurosci *38*, 6102-6113. 10.1523/jneurosci.3350-17.2018.

Costa-Mattioli, M., Gobert, D., Harding, H., Herdy, B., Azzi, M., Bruno, M., Bidinosti, M., Ben Mamou, C., Marcinkiewicz, E., Yoshida, M., et al. (2005). Translational control of hippocampal synaptic plasticity and memory by the eIF2alpha kinase GCN2. Nature *436*, 1166-1173. 10.1038/nature03897.

Di Prisco, G., Huang, W., Buffington, S., Hsu, C., Bonnen, P., Placzek, A., Sidrauski, C., Krnjević, K., Kaufman, R., Walter, P., and Costa-Mattioli, M. (2014). Translational control of mGluR-dependent long-term depression and object-place learning by eIF2α. Nat Neurosci *17*, 1073-1082.

Downs, A.M., Fan, X., Kadakia, R.F., Donsante, Y., Jinnah, H.A., and Hess, E.J. (2021). Cell-intrinsic effects of TorsinA(ΔE) disrupt dopamine release in a mouse model of TOR1A dystonia. Neurobiol Dis *155*, 105369. 10.1016/j.nbd.2021.105369.
Elvira, R., Cha, S.J., Noh, G.M., Kim, K., and Han, J. (2020). PERK-Mediated eIF2α Phosphorylation Contributes to The Protection of Dopaminergic Neurons from Chronic Heat Stress in Drosophila. Int J Mol Sci *21*. 10.3390/ijms21030845.
Emery, P. (2007). Protein extraction from Drosophila heads. Methods Mol Biol *362*, 375-377. 10.1007/978-1-59745-257-1_27.
Eskow Jaunarajs, K.L., Bonsi, P., Chesselet, M.F., Standaert, D.G., and Pisani, A. (2015). Striatal cholinergic dysfunction as a unifying theme in the pathophysiology of dystonia. Prog Neurobiol *127-128*, 91-107. 10.1016/j.pneurobio.2015.02.002.
Estes, P., Boehringer, A., Zwick, R., Tang, J., Grigsby, B., and Zarnescu, D. (2011). Wild-type and A315T mutant TDP-43 exert differential neurotoxicity in a Drosophila model of ALS. Hum Mol Genet *20*, 2308-2321.
Fremont, R., Tewari, A., and Khodakhah, K. (2015). Aberrant Purkinje cell activity is the cause of dystonia in a shRNA-based mouse model of Rapid Onset Dystonia-Parkinsonism. Neurobiol Dis *82*, 200-212. 10.1016/j.nbd.2015.06.004.
García, M.A., Meurs, E.F., and Esteban, M. (2007). The dsRNA protein kinase PKR: virus and cell control. Biochimie *89*, 799-811. 10.1016/j.biochi.2007.03.001.
Girardin, S.E., Cuziol, C., Philpott, D.J., and Arnoult, D. (2021). The eIF2α kinase HRI in innate immunity, proteostasis, and mitochondrial stress. Febs j *288*, 3094-3107. 10.1111/febs.15553.
Karam, C.S., Jones, S.K., and Javitch, J.A. (2020). Come Fly with Me: An overview of dopamine receptors in Drosophila melanogaster. Basic Clin Pharmacol Toxicol *126 Suppl 6*, 56-65. 10.1111/bcpt.13277.
Karimi, M., and Perlmutter, J.S. (2015). The role of dopamine and dopaminergic pathways in dystonia: insights from neuroimaging. Tremor Other Hyperkinet Mov (N Y) *5*, 280. 10.7916/d8j101xv.
Kilberg, M.S., Shan, J., and Su, N. (2009). ATF4-dependent transcription mediates signaling of amino acid limitation. Trends Endocrinol Metab *20*, 436-443. 10.1016/j.tem.2009.05.008.
Kim, M., Sandford, E., Gatica, D., Qiu, Y., Liu, X., Zheng, Y., Schulman, B., Xu, J., Semple, I., Ro, S., et al. (2016). Mutation in ATG5 reduces autophagy and leads to ataxia with developmental delay. eLife *5*, e12245.
Kitamoto, T. (2001). Conditional modification of behavior in Drosophila by targeted expression of a temperature-sensitive shibire allele in defined neurons. J Neurobiol *47*, 81-92. 10.1002/neu.1018.
Koh, Y., Rehfeld, K., and Ganetzky, B. (2004). A Drosophila model of early onset torsion dystonia suggests impairment in TGF-beta signaling. Hum Mol Genet *13*, 2019-2030.
Kuipers, D.J.S., Mandemakers, W., Lu, C.S., Olgiati, S., Breedveld, G.J., Fevga, C., Tadic, V., Carecchio, M., Osterman, B., Sagi-Dain, L., et al. (2021). EIF2AK2 Missense Variants Associated with Early Onset Generalized Dystonia. Ann Neurol *89*, 485-497. 10.1002/ana.25973.
Lester, D.B., Rogers, T.D., and Blaha, C.D. (2010). Acetylcholine-dopamine interactions in the pathophysiology and treatment of CNS disorders. CNS Neurosci Ther *16*, 137-162. 10.1111/j.1755-5949.2010.00142.x.
Lewis, S.A., Bakhtiari, S., Forstrom, J., Bayat, A., Bilan, F., Le Guyader, G., Alkhunaizi, E., Vernon, H., Padilla-Lopez, S.R., and Kruer, M.C. (2023). AGAP1-associated endolysosomal trafficking abnormalities link gene-environment interactions in a neurodevelopmental disorder. bioRxiv. 10.1101/2023.01.31.526497.
Liu, J., Pasini, S., Shelanski, M.L., and Greene, L.A. (2014). Activating transcription factor 4 (ATF4) modulates post-synaptic development and dendritic spine morphology. Front Cell Neurosci *8*, 177. 10.3389/fncel.2014.00177.

Longo, F., Mancini, M., Ibraheem, P.L., Aryal, S., Mesini, C., Patel, J.C., Penhos, E., Rahman, N., Mamcarz, M., Santini, E., et al. (2021). Cell-type-specific disruption of PERK-eIF2α signaling in dopaminergic neurons alters motor and cognitive function. Mol Psychiatry *26*, 6427-6450. 10.1038/s41380-021-01099-w.
Ly, S., Lee, D.A., Strus, E., Prober, D.A., and Naidoo, N. (2020). Evolutionarily Conserved Regulation of Sleep by the Protein Translational Regulator PERK. Curr Biol *30*, 1639-1648.e1633. 10.1016/j.cub.2020.02.030.
Maltese, M., Stanic, J., Tassone, A., Sciamanna, G., Ponterio, G., Vanni, V., Martella, G., Imbriani, P., Bonsi, P., Mercuri, N., et al. (2018). Early structural and functional plasticity alterations in a susceptibility period of DYT1 dystonia mouse striatum. Elife *7*, e33331.
Malzer, E., Daly, M.L., Moloney, A., Sendall, T.J., Thomas, S.E., Ryder, E., Ryoo, H.D., Crowther, D.C., Lomas, D.A., and Marciniak, S.J. (2010). Impaired tissue growth is mediated by checkpoint kinase 1 (CHK1) in the integrated stress response. J Cell Sci *123*, 2892-2900. 10.1242/jcs.070078.
Malzer, E., Szajewska-Skuta, M., Dalton, L.E., Thomas, S.E., Hu, N., Skaer, H., Lomas, D.A., Crowther, D.C., and Marciniak, S.J. (2013). Coordinate regulation of eIF2α phosphorylation by PPP1R15 and GCN2 is required during Drosophila development. J Cell Sci *126*, 1406-1415. 10.1242/jcs.117614.
Mao, D., Reuter, C.M., Ruzhnikov, M.R.Z., Beck, A.E., Farrow, E.G., Emrick, L.T., Rosenfeld, J.A., Mackenzie, K.M., Robak, L., Wheeler, M.T., et al. (2020). De novo EIF2AK1 and EIF2AK2 Variants Are Associated with Developmental Delay, Leukoencephalopathy, and Neurologic Decompensation. Am J Hum Genet *106*, 570-583. 10.1016/j.ajhg.2020.02.016.
Martin, J.R., Ernst, R., and Heisenberg, M. (1998). Mushroom bodies suppress locomotor activity in Drosophila melanogaster. Learn Mem *5*, 179-191.
Neill, G., and Masson, G.R. (2023). A stay of execution: ATF4 regulation and potential outcomes for the integrated stress response. Front Mol Neurosci *16*, 1112253. 10.3389/fnmol.2023.1112253.
Nelson, A.B., Girasole, A.E., Lee, H.Y., Ptáček, L.J., and Kreitzer, A.C. (2022). Striatal Indirect Pathway Dysfunction Underlies Motor Deficits in a Mouse Model of Paroxysmal Dyskinesia. J Neurosci *42*, 2835-2848. 10.1523/jneurosci.1614-20.2022.
Niethammer, M., Carbon, M., Argyelan, M., and Eidelberg, D. (2011). Hereditary dystonia as a neurodevelopmental circuit disorder: Evidence from neuroimaging. . Neurobiol Dis *42*, 202-209.
Pakos-Zebrucka, K., Koryga, I., Mnich, K., Ljujic, M., Samali, A., and Gorman, A. (2016). The integrated stress response. EMBO Rep *17*, 1374-1395. 10.15252/embr.201642195.
Peng, I.F., Berke, B.A., Zhu, Y., Lee, W.H., Chen, W., and Wu, C.F. (2007). Temperature-dependent developmental plasticity of Drosophila neurons: cell-autonomous roles of membrane excitability, Ca2+ influx, and cAMP signaling. J Neurosci *27*, 12611-12622. 10.1523/jneurosci.2179-07.2007.
Pohl, C., Happe, J., and Klockgether, T. (2002). Cooling improves the writing performance of patients with writer's cramp. Mov Disord *17*, 1341-1344.
Reenan, R.A., and Rogina, B. (2008). Acquired temperature-sensitive paralysis as a biomarker of declining neuronal function in aging Drosophila. Aging Cell *7*, 179-186. 10.1111/j.1474-9726.2008.00368.x.
Rittiner, J., Caffall, Z., Hernández-Martinez, R., Sanderson, S., Pearson, J., Tsukayama, K., Liu, A., Xiao, C., Tracy, S., Shipman, M., et al. (2016). Functional Genomic Analyses of Mendelian and Sporadic Disease Identify Impaired eIF2α Signaling as a Generalizable Mechanism for Dystonia. Neuron *92*, 1238-1251.
Ron, D., and Walter, P. (2007). Signal integration in the endoplasmic reticulum unfolded protein response. Nat Rev Mol Cell Biol *8*, 519-529. 10.1038/nrm2199.
Sabandal, P.R., Saldes, E.B., and Han, K.A. (2022). Acetylcholine deficit causes dysfunctional inhibitory control in an aging-dependent manner. Sci Rep *12*, 20903. 10.1038/s41598-022-25402-z.
Simonyan, K., Cho, H., Hamzehei Sichani, A., Rubien-Thomas, E., and Hallett, M. (2017). The direct basal ganglia pathway is hyperfunctional in focal dystonia. Brain *140*, 3179-3190. 10.1093/brain/awx263.

Smith, S.G., Haynes, K.A., and Hegde, A.N. (2020). Degradation of Transcriptional Repressor ATF4 during Long-Term Synaptic Plasticity. Int J Mol Sci *21*. 10.3390/ijms21228543.
Sonenberg, N., and Hinnebusch, A.G. (2009). Regulation of translation initiation in eukaryotes: mechanisms and biological targets. Cell *136*, 731-745. 10.1016/j.cell.2009.01.042.
Song, C.H., Bernhard, D., Bolarinwa, C., Hess, E.J., Smith, Y., and Jinnah, H.A. (2013). Subtle microstructural changes of the striatum in a DYT1 knock-in mouse model of dystonia. Neurobiol Dis *54*, 362-371. 10.1016/j.nbd.2013.01.008.
Thenganatt, M.A., and Jankovic, J. (2014). Treatment of dystonia. Neurotherapeutics *11*, 139-152. 10.1007/s13311-013-0231-4.
Tsuyama, T., Tsubouchi, A., Usui, T., Imamura, H., and Uemura, T. (2017). Mitochondrial dysfunction induces dendritic loss via eIF2α phosphorylation. J Cell Biol *216*, 815-834.
Valenzuela, V., Oñate, M., Hetz, C., and Court, F. (2016). Injury to the nervous system: A look into the ER. Brain Res *1648*, 617-625.
Vo, A., Sako, W., Niethammer, M., Carbon, M., Bressman, S., Uluğ, A., and Eidelberg, D. (2015). Thalamocortical Connectivity Correlates with Phenotypic Variability in Dystonia. Cereb Cortex *25*, 3086-3094.
von Spiczak, S., Helbig, K.L., Shinde, D.N., Huether, R., Pendziwiat, M., Lourenço, C., Nunes, M.E., Sarco, D.P., Kaplan, R.A., Dlugos, D.J., et al. (2017). DNM1 encephalopathy: A new disease of vesicle fission. Neurology *89*, 385-394. 10.1212/wnl.0000000000004152.
Wakabayashi-Ito, N., Ajjuri, R.R., Henderson, B.W., Doherty, O.M., Breakefield, X.O., O'Donnell, J.M., and Ito, N. (2015). Mutant human torsinA, responsible for early-onset dystonia, dominantly suppresses GTPCH expression, dopamine levels and locomotion in Drosophila melanogaster. Biol Open *4*, 585-595. 10.1242/bio.201411080.
Wang, Z., Gao, C., Chen, W., Gao, Y., Wang, H., Meng, Y., Luo, C., Zhang, M., Chen, G., Chen, X., et al. (2019). Salubrinal offers neuroprotection through suppressing endoplasmic reticulum stress, autophagy and apoptosis in a mouse traumatic brain injury model. Neurobiol Learn Mem *161*, 12-25.
Young, S.K., and Wek, R.C. (2016). Upstream Open Reading Frames Differentially Regulate Gene-specific Translation in the Integrated Stress Response. J Biol Chem *291*, 16927-16935. 10.1074/jbc.R116.733899.
Zakirova, Z., Fanutza, T., Bonet, J., Readhead, B., Zhang, W., Yi, Z., Beauvais, G., Zwaka, T., Ozelius, L., Blitzer, R., et al. (2018). Mutations in THAP1/DYT6 reveal that diverse dystonia genes disrupt similar neuronal pathways and functions. PLoS Genet *14*, e1007169.
Zech, M., Castrop, F., Schormair, B., Jochim, A., Wieland, T., Gross, N., Lichtner, P., Peters, A., Gieger, C., Meitinger, T., et al. (2014). DYT16 revisited: exome sequencing identifies PRKRA mutations in a European dystonia family. Mov Disord *29*, 1504-1510.
Zhou, F.M., Liang, Y., and Dani, J.A. (2001). Endogenous nicotinic cholinergic activity regulates dopamine release in the striatum. Nat Neurosci *4*, 1224-1229. 10.1038/nn769.
Zyryanova, A.F., Kashiwagi, K., Rato, C., Harding, H.P., Crespillo-Casado, A., Perera, L.A., Sakamoto, A., Nishimoto, M., Yonemochi, M., Shirouzu, M., et al. (2021). ISRIB Blunts the Integrated Stress Response by Allosterically Antagonising the Inhibitory Effect of Phosphorylated eIF2 on eIF2B. Mol Cell *81*, 88-103.e106. 10.1016/j.molcel.2020.10.031.

Supplemental Materials

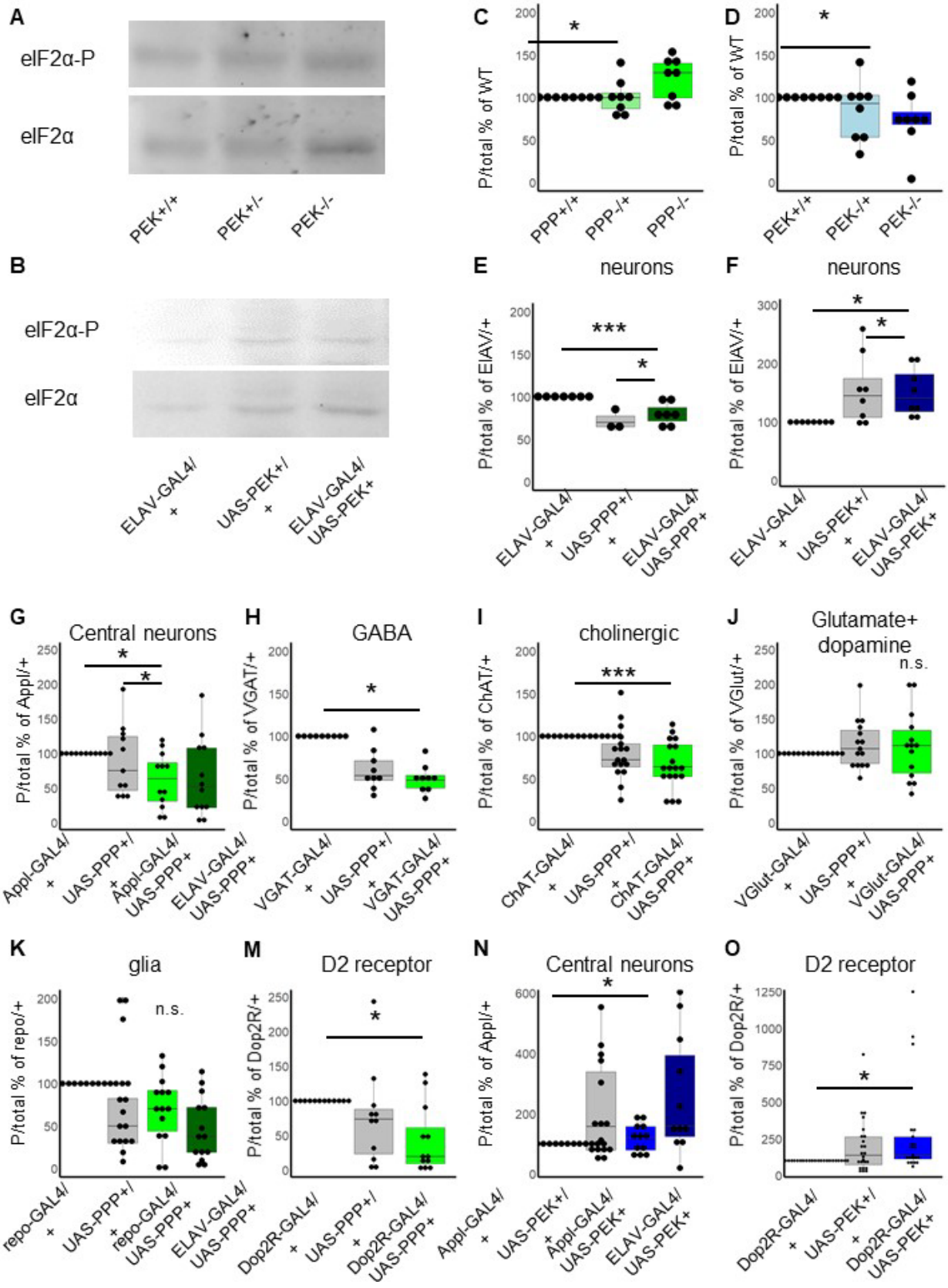

Supplemental Figure 1: Alterations to eIF2a-P confirmed by western blotting. Green represents alterations to the PPP151R phosphatase (PPP), which removes phosphorylation from eIF2α (eIF2α-P). Blue represents the PERK kinase (PEK) which phosphorylates eIF2α-P. A-B, sample images of western blots. C-D. Quantification of ratios of phosphorylated/total eIF2α normalized to homozygous genetic background line (yw) for whole-animals collected at 14 days post-eclosion with loss-of-function variants in PPP (C) and PEK (D). Decreasing PPP increases ratios of eIF2α-P and decreasing PEK decreases ratios of eIF2α-P. E-O Quantification of ratios of phosphorylated/total eIF2α normalized to Gal4/+ heterozygous control taken from adult heads 14 days post-eclosion. E-F. Neuron-specific overexpression of PPP increases eIF2α-P (E) and PEK decreases eIF2α-P (F). G-M Overexpression of PPP in Gal4 lines decreases eIF2α-P and reaches significance in central (G), GABA (H), cholinergic (I), and D2 receptor (M) neurons. Non-significance is thought to be due to small anatomical regions of overexpression. N-O. Overexpression of PEK in Gal-4 lines significantly increases eIF2α-P in central (N) and D2-receptor (O) containing neurons. Dop1R n.s. (not shown).

Supplemental Table 1

Genotype abbreviation	Localization/timing	Genotype	Source
w1118	whole animal	w^{1118} crossed with Canton S and backcrossed for 12 generation	BDSC 3605
y w	whole animal	y w	BDSC 6598
CantonS	whole animal	wild-type (+)	BDSC 64349
PPP-	whole animal	yw; P[w+]PPP1R15^{G18907} 2nd 5' insertion (UAS mis-expression element)	BDSC 26945
PEK-	whole animal	yw; PEK^{EY09578} 3rd 5' insertion (UAS mis-expression element)	BDSC 17582
ELAV	Post mitotic neurons, embryonic-adult	w*; P[GAL4-elav.L] 3rd	BDSC 8760
Appl	Neurons, central brain> VNC>salivary glands+fat	P[Appl-Gal4.G1a]1, y w* 1st	BDSC 32040

	body. higher in males. Larva-adult.		
VGlut	Synaptic vesicle transporter in terminals of glutamatergic and dopaminergic neurons	TI[2A-GAL4]VGlut2A-GAL4/CyO 2nd	BDSC 84697
Dop1R	Dopamine receptor GPCR; gamma Kenyon cell, adult MB, central complex (basal ganglia homologous structure), optic lobe	w1118; P[GMR72B08-GAL4] attP2 3rd	BDSC 46669
Dop2R	Dopamine receptor GPCR; nervous, digestive, excretory systems. Pre 3rd instar larva expression. Higher in males.	w* TI[2A-GAL4]Dop2R2A-GAL4 1st	BDSC 84628
repo	glia. Embryonic-adult	w1118; P[GAL4]repo/TM3, Sb 3rd	BDSC 7415
VGat	GABA vesicle transport; inhibitory interneurons, embryonic-adult	w*; P[VGAT-GAL4.F] 3rd	BDSC 58409
ChAT	Choline acetyltransferase; excitatory neurons, embryonic-adult	TI[2A-GAL4]ChAT2A-GAL4/TM3, Sb 3rd	BDSC 84618
OK6	motor neurons, embryonic-adult	P[GawB]OK6 2nd	BDSC 64199
OK107	MB neurons + neuroblasts, larval-adult	w; P[eyOK107/In(4)ciD, panclD, sspa-pol 4th	BDSC 854
PPP+	UAS-driven (Gal4 cell-specific)	M[UAS-PPP1R15.ORF.3xHA.GW]ZH-86Fb 3rd	Fly ORF F003018
PEK+	UAS-driven (Gal4 cell-specific)	w1118; P[UAS-PEK.M]3/TM6B, Tb 3rd	BDSC 76248

ATF4+	UAS-driven (Gal4 cell-specific)	M[UAS-crc.ORF.3xHA.GW]ZH-86Fb 3rd	Fly ORF F000106
htorΔE	UAS-driven (Gal4 cell-specific)	w-; P[w+, UAS-htorADeltaE]#24 2nd	Naoto Ito (Wakabayashi-Ito et al., 2015)
htorA	UAS-driven (Gal4 cell-specific)	w-; P[w+, UAS-htorA]#8 2nd	Naoto Ito (Wakabayashi-Ito et al., 2015)
shibire^{ts-1}	UAS-driven (Gal4 cell-specific)	w*; P[UAS-shits1.K]3	BDSC 442222

Supplemental table 1: Drosophila lines used in studies. BDSC=Bloomington Drosophila Stock Center. VNC=ventral nerve cord (spinal cord analogue). MB=Mushroom bodies. GPCR=G-coupled protein receptor.

Supplemental Table 2

Antibody/stain	Species	Concentration	Application	Company	Lot(s) #
DLG	M	1:400	NMJ IHC	DSHB 4F3	2/18/16
Anti-mouse Cy3	G	1:400	NMJ IHC	ThermoFisher	A10521 1425618
Anti-HRP 647	G	1:100	NMJ IHC	Jackson Immuno Research	126323
Phalloidin 488	-	1:300	NMJ IHC	Molecular Probes	1903540 2160010
Beta actin	M	1:2000	WB	Abcam 8224	GR14272-3
Beta tubulin	R	1:2000	WB	Abcam 6046	GR3376491-1
Phosphor-S51 eIF2S	R	1:1000	WB	Cell Signaling 3597	12
eIF2S1	R	1:500	WB	Abcam 26197	GR3183673-1 GR3325905
Rabbit ECL	G	1:10000	WB	GE healthcare NA931	17473046
Mouse ECL	G	1:10000	WB	GE Healthcare NA934	17170583

Supplemental Table 2: Antibodies used in studies. HRP=horseradish peroxidase (recognizes nirvana2 neuronal surface protein in Drosophila), ECL= Enhanced Chemiluminescence, M=mouse, G=goat, R=rabbit. NMJ IHC=neuromuscular junction immunohistochemistry, WB=western blot

Supplemental Table 3

Software	Library/ function	Company	Source
R/R studio (v. 4.2.2)	Survival, tidyverse, irrCAC	The R project for Statistical Computing	https://cran.r-project.org/bin/windows/base/
ImageJ software v. 1.50i	measure distance/ area	National Institutes of Health	https://imagej.nih.gov/ij/download.html
Photoshop	image stitching	Adobe	https://www.adobe.com/products/photoshop.html
Premier Pro/Rush	frame-by-frame video analysis	Adobe	https://www.adobe.com/products/premiere.html
Image studio Lite	western signal quantification	LiCor	https://www.licor.com/bio/image-studio-lite/
Zen Black/blue	confocal imaging and projections	Zeiss	https://www.zeiss.com/microscopy/en/products/software/zeiss-zen-lite.html

Supplemental Table 3: Software used in studies